Clinical and Translational Radiation Oncology 53 (2025) 100965

Contents lists available at ScienceDirect

Clinical and Translational Radiation Oncology

journal homepage: www.sciencedirect.com/journal/clinical-and-translational-radiation-oncology

Original Research Article

Pre-Treatment and Pre-Brachytherapy MRI first-order Radiomic Features by a Commercial software as survival predictors in radiotherapy for cervical cancer Objectives

Wiwatchai Sittiwong [a], Pittaya Dankulchai [a,*], Pitchayut Wongsuwan [a], Tissana Prasartseree [a], Wajana Thaweerat [a], Nerisa Thornsri [b], Pongpop Tuntapakul [a]

[a] Division of Radiation Oncology, Department of Radiology, Faculty of Medicine Siriraj Hospital, Mahidol University, Bangkok, Thailand
[b] Research Unit, Faculty of Medicine Siriraj Hospital, Bangkok, Thailand

ARTICLE INFO

Keywords:
MR radiomics
Cervical cancer
3D-IGABT
Prediction models
Nomograms
Survival outcomes

ABSTRACT

Materials and Methods: The study included 100 patients with LACC who underwent definitive CCRT with IMRT/VMAT technique followed by 3D-IGABT. MRI-based contouring included T2WI and DWI images for primary tumor (GTVp) and lymph nodes (GTVn). The contours were imported to MIM software to extract first-order radiomic features. Radiomic values from pre-treatment (PreRx), pre-brachytherapy (PreBT), differences between PreRx and PreBT (Diff) radiomic and clinical factors were analyzed using univariate and multivariate Cox regression analysis. Predictive models of PFS, LRFS, DMFS, and OS were created along with the optimism index and calibration plot.

Results: The median follow-up time was 24.5 months. The 2-year of PFS, LRFS, DMFS, and OS rates were 71, 88.6, 83.1, and 83.5 %, respectively. For all clinical outcomes, CF + RF combined from PreRx and PreBT resulted in the highest Harrell's C-index compared with the CF or RF alone. Compare with Diff models, models from PreRx and PreBT resulted in higher Harrell's C-index. The C-indexes from the CF + RF model from PreRx and PreBT for PFS, LRFS, DMFS, and OS were 0.739, 0.873, 0.830 and 0.967 with the optimism indexes of 0.312, 0.381, 0.316, and 0.242, respectively.

Conclusion: Radiomic features from the first-order statistics added values to clinical factors to predict the outcomes after CCRT. The highest prediction model performance was for the combined clinical and radiomics from PreRx and PreBT.

Introduction

The current standard treatment for locally advanced cervical cancer (LACC) includes concurrent chemoradiation (CCRT) followed by three-dimensional image-guided adaptive brachytherapy (3D-IGABT). Several studies have shown that 3D-IGABT has favorable treatment outcomes with an acceptable toxicity rate [1–5]. Findings from the EMBRACE-I [2] study, which focused on patients with LACC treated with brachytherapy using MRI-guided adaptive techniques, determined that the 5-year local control rate ranged from 89–100 %. These results indicated highly satisfactory treatment outcomes. However, the 5-year disease-free survival (DFS) rates ranged from 47–76 %, suggesting that preventing disease recurrence was challenging. Analysis from the RetroEMBRACE[1] study demonstrated that treatment failure, particularly distant metastasis, was the most frequent relapse and predominant within the first-year post-treatment. This raises questions on the adequacy of the current standard treatment for LACC, considering the role of adjuvant chemotherapy.

Adjuvant systemic therapy in LACC has been evaluated in several phase 3 randomized trials. OUTBACK[6] trial demonstrated no benefit of adjuvant chemotherapy towards DFS or overall survival (OS) compared to CCRT alone. Although, another randomized study by Dueñas-González et al.[7] revealed that the adjuvant chemotherapy arm had superior progression-free survival (PFS), OS, and fewer distant metastases compared to standard CCRT. This approach led to significantly higher grade 3–5 adverse events. However, adjuvant

* Corresponding author at: Division of Radiation Oncology, Department of Radiology, Faculty of Medicine Siriraj Hospital, 2 Wanglang Rd., Siriraj, Bangkok Noi, Bangkok, 10700, Thailand.
E-mail address: pittaya.dan@mahidol.ac.th (P. Dankulchai).

https://doi.org/10.1016/j.ctro.2025.100965
Received 28 April 2024; Received in revised form 18 January 2025; Accepted 15 April 2025
Available online 19 April 2025

immunotherapy with pembrolizumab has demonstrated benefits in improving progression-free survival (PFS) following CCRT.[8] Similarly, neoadjuvant chemotherapy has been shown to significantly enhance both PFS and overall survival (OS) in patients with LACC.[9] Given the substantial risk of distant metastasis, adjuvant or neoadjuvant systemic therapy should be considered for patients at high risk of distant relapse. However, a reliable and robust tool for identifying suitable patients has yet to be established.

Numerous studies have attempted to identify factors that predict the prognosis in patients with LACC [11–13,26]. Advancements in technology, including artificial intelligence (AI), have led to widespread research in radiomics. Radiomic features (RF) obtained from data extraction and conversion into measurable quantitative information could be analyzed for prognostic purposes. The prognostic value of radiomics was previously shown in several diseases including cervical cancer, which aids clinicians in personalizing treatment for individual patients.[14–20] A study by Zhang et al.[21] extracted 400 MRI-based RF from 185 patients with LACC and found that RF could effectively predict OS and DFS rates better than FIGO staging. Treatment response post-CCRT in LACC can be predicted by MR radiomics. The study from Ikushima et al[22] demonstrated that combining MRI radiomics with clinical parameters improved the accuracy of predicting out-of-field recurrence (OFR) post-CCRT for LACC.

However, all studies to date have focused solely on RF extracted from MRI from PreRx images. A change of parameters for images during or after treatment may provide more information. Meng J et al.[15] prospectively analyzed 32 patients with cervical cancer who underwent diffusion weighted MRI pre-CCRT, at the end of the 2nd and 4thweek during CCRT and immediately after CCRT. The results showed that RF was changed significantly during radiation and could be used for monitoring early tumor response. Therefore, in patients with cervical cancer, analyzing RF from pre-treatment (PreRx) MRI, pre-brachytherapy (PreBT) MRI, and RF changes between PreRx and PreBT could add more prognostic value. This study aimed to investigate the significance of MR radiomics to predict the treatment outcome in patients with LACC after definitive CCRT and 3D-IGABT.

Materials and methods

Study Designs and Participants

The study included 100 patients who were treated between 2016 and 2022 were retrospectively analyzed. The inclusion criteria were patients diagnosed with LACC of any histologic subtype who underwent CCRT. Eligible patients had to undergo intensity modulated radiation therapy (IMRT)/volumetric modulated arc therapy (VMAT) technique, and 3D-IGABT. PreRx and PreBT MRI assessments were mandatory. Participants had to have imaging evaluations of lower abdomen using MRI at 3 months post-treatment. The patients were excluded should they have had an incomplete image dataset. Additionally, patients with incomplete radiotherapy sessions, adjuvant chemotherapy after CCRT, and a history of trachelectomy, hysterectomy, or radical hysterectomy, history of secondary malignancy, previous pelvic radiotherapy, or previous chemotherapy were also excluded. This study was approved by the Institutional Review Board (xxx/xxxx).

Contouring and MR-RF extraction

Target delineation of primary tumor (GTVp) and pathologic lymph nodes (GTVn) was done on Eclipse® software from Varian, A Siemens Healthineers Company. Pathologic lymph nodes were determined based on lymph nodes with a size $\geq$ 1 cm in the short axis or those that exhibited suspicious morphology. For all patients, contours were created for PreRx and PreBT imaging on T2WI and DWI. Subsequently, all MR images were imported to MIM®software, and first-order RF were extracted based on the available standard function provided by the software. The data was categorized to PreRx, PreBT radiomics, and the Diff of radiomics between PreRx and PreBT of GTVp and GTVn for T2WI and DWI. The study cohort is presented as Fig. 1.

Statistical analysis

A total of 120 radiomic values from PreRx, PreBT, Diff radiomics, and 20 CF from 100 patients were analyzed. Chi-square and Mann Whitney-U tests compared the differences in CF/RF, and clinical outcomes. Factors with P-values < 0.1 were included for multivariate analysis. Multivariate analysis was conducted using Cox-regression analysis. P-values < 0.05 were considered to be statistically significant. Significant variables from multivariate analysis were entered in the prediction model of each outcome. The predictive performance of the prediction model was evaluated by Harrell's C-index. C-index of 0.50–0.70 represented poor accuracy; 0.71–0.90 represented moderate accuracy; >0.90 represented high accuracy. Optimism on predictive indices using Bootstrap samples for internal validation of the model was performed. The predictive performance of the model to predict the events against actual events was shown as a calibration plot. The Cox regression models to quantify the probability of PFS and DMFS was transformed into nomograms.

Results

Patient and treatment characteristics

The median follow-up time was 24.5 months (interquartile range [IQR] 19.9–31.2).

According to the FIGO 2018 staging, most patients were classified as stage IIIC1r (52 %) and stage IIIC2r (21 %). All patients underwent definitive CCRT with the dose to whole pelvis of 44–50.4 Gy in 20–28 fractions with or without lymph nodes simultaneous integrated boost to 53–60 Gy. 3D-IGABT was performed in every patient and the mean D90 HR-CTV dose was 89.94 Gy (SD 5.81) EQD2 ($\alpha/\beta = 10$; Gy10). Baseline patient characteristics and treatment characteristics are shown in Table 1. Significant CF and RF from univariate analysis were shown in Supplementary Table S1.

PFS

The median time to any progression was 21.8 months (IQR 15.2–30.5), the rate of 2-years of PFS was 71.0 % (95 % confidence

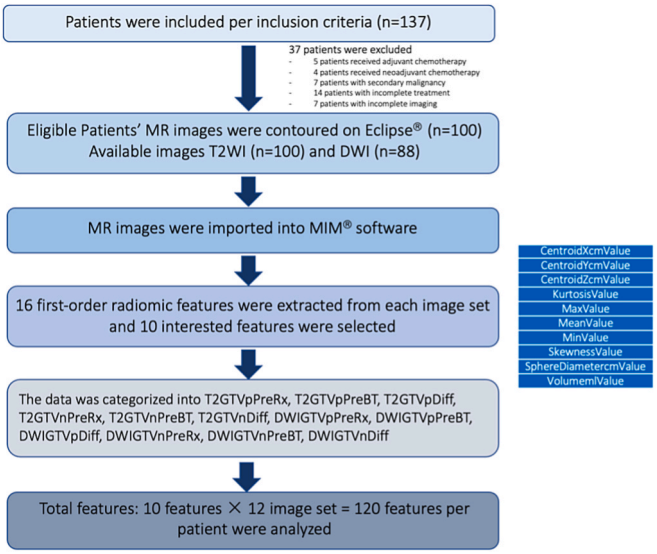

Fig. 1.

Table 1
Baseline patient characteristics and treatment characteristics (N = 100).

Patient characteristics Characteristics	Numbers (%)	Treatment characteristics Characteristics	Numbers (%)
Age (years)		**Field**	
< 40	18 (18 %)	Whole pelvis	66 (66 %)
40—60	50 (50 %)	Whole pelvis and PAN field	34 (34 %)
> 60	32 (32 %)		
Pre-treatment		**D_{95} CTV whole pelvis**	
Hemoglobin (g/dL)	82 (82 %)	Mean, Gy [SD]	45.93 [2.60]
≥ 10	18 (18 %)		
< 10			
HIV status		**D_{95} CTV LN boost**	
Negative	99 (99 %)	Mean, Gy [SD]	58.15 [2.61]
Positive	1 (1 %)		
FIGO2018 staging		**Primary tumor dose received before brachytherapy**	
IIA2	1 (1 %)		
IIB	9 (9 %)	Mean, Gy [SD]	36.44 [5.99]
IIIA	1 (1 %)		
IIIB	8 (8 %)		
IIIC1r	52 (52 %)		
IIIC2r	21 (21 %)		
IVA	8 (8 %)		
AJCC 9th T staging		**Pathologic LN dose received before brachytherapy**	
T1b2	2 (2 %)		
T1b3	6 (6 %)		45.12 [7.47]
T2a2	3 (3 %)	Mean, Gy [SD]	
T2b	37 (37 %)		
T3a	1 (1 %)		
T3b	43 (43 %)		
T4	8 (8 %)		
AJCC 9th N staging		**D_{90} HR-CTV**	
N0	19 (19 %)	Mean, Gy [SD]	89.94 [5.81]
N1	54 (54 %)		
N2	27 (27 %)		
Pathology		**Brachytherapy Technique**	
Squamous Cell	72 (72 %)		13 (13 %)
Carcinoma	23 (23 %)	Intracavitary	87 (87 %)
Adenocarcinoma	4 (4 %)	Intracavitary and Interstitial	
Adenosquamous	1 (1 %)		
Others			
Differentiation		**Chemotherapy Regimen**	
Well	8 (8 %)		87 (87 %)
Moderate	67 (67 %)	Cisplatin	8 (8 %)
Poor	10 (10 %)	Carboplatin	5 (5 %)
Unknown	15 (15 %)	Cisplatin and Carboplatin	
Number of Pelvic LN (N = 81)	31 (38.3 %)	**Cumulative Cisplatin Dose (mg/m^2)**	15 (15 %)
1–3	24 (29.6 %)	0—50	5 (5 %)
4–6	10 (12.3 %)	> 50—100	10 (10 %)
7–9	16 (19.8 %)	> 100—150	70 (70 %)
≥ 10		> 150	
Maximum short axis diameter of pathologic LN (N = 81) Mean, cm [SD]	1.17 [0.49]	**Total Treatment Time** Median, days [IQR]	47.5 [44–54]
Number of LN size ≥ 1 cm (N = 81)	34 (42.0 %)	**MRI Interval** Median, days [IQR]	29 [26–33]
0	34 (42.0 %)		
1–3	10 (12.3 %)		
4–6	3 (3.7 %)		
≥ 7			
Number of Necrotic LN (N = 81)	24 (29.6 %)	**T category at pre-brachytherapy***	38(38 %)
0	35 (43.2 %)	I	42(42 %)
1–3	18 (22.2 %)	II	13(13 %)
4–6	4 (5.0 %)	III	7(7 %)
≥ 7		IV	

*According to IBS-GEC ESTRO-ABS recommendations.

interval [CI] 60.35–79.30). The Kaplan-Meier curve of PFS is shown in Fig. 2a. Thirty patients had the most common progression which is distant metastasis (63.3 %). Univariate Cox regression analysis results for PFS are shown in Supplementary Table S2 and S6. The Cox regression CF + RF model in PreRx and PreBT resulted in the highest Harrell's C-index of 0.739; and the Harrell's Cindices of the models from RF and CF alone were 0.689 and 0.565, respectively. The optimism index of the CF + RF model was 0.438. The calibration plot of the CF + RF model to predict any progression, was underestimated and overestimated when predicting low probabilities but was closer to the reference line when predicting high probabilities (Fig. 3a). For Diff radiomics multivariate analysis, no significant CF were found, and the Harrell's C-index from RF alone was 0.588 with an optimism index of 0.312. The performance of the Diff radiomics model was lower than the PreRx and PreBT models. The Cox regression models for PFS from the CF + RF of PreRx/PreBT and Diff are shown in Table 2.

LRFS

The median time to local recurrence was 22.9 months (IQR 18.2–30.8). Ten patients developed local recurrence and the rate of 2-years of LRFS was 88.6 % (95 % CI 79.62–93.82). The Kaplan-Meier curve of LRFS is shown in Fig. 2b. Univariate Cox regression analysis for LRFS is shown in Supplementary Table S3 and S7. The CF + RF Cox regression model from PreRx and PreBT yielded the highest Harrell's C-index of 0.873 compared to the Harrell's C-indices of the models from RF and CF alone, 0.824 and 0.705, respectively. The optimism index of the CF + RF model was 0.472. The model's calibration plot underestimated when predicting low probabilities and overestimated when predicting high probabilities with larger magnitude from the reference line, indicating the uncertainty of the model's predive performance (Fig. 3b). For Diff radiomics multivariate analysis, no significant CF were found, and the Harrell's C-index from RF alone was 0.773 with the optimism index of 0.381 which represented poorer accuracy of LRFS prediction compared to the CF + RF model from PreRx and PreBT. The Cox regression models for PFS from CF + RF of PreRx/PreBT and Diff are shown in Table 2.

DMFS

The median time to distant metastasis was 22.7 months (IQR 18.3–30.8) and the rate of 2-years of DMFS was 83.1 % (95 % CI 73.67–89.38). The Kaplan-Meier curve of DMFS was shown in Fig. 2c. From 19 patients that underwent distant relapse, the most common sites of distant metastasis were supraclavicular lymph node (19 %), intra-abdominal lymph node (14 %), and lung (12 %). Univariate Cox regression analysis for DMFS is shown in Supplementary Table S4 and S8. The Cox regression CF + RF model from PreRx and PreBT had the highest Harrell's C-index of 0.830 with optimism index of 0.292. Harrell's C-indices of the models from RF and CF alone were 0.803 and 0.720, respectively. The calibration plot of the CF + RF model underestimated when predicting low probabilities and overestimated when predicting high probabilities, however the trend still corresponded to the reference line, (Fig. 3c). For Diff radiomics multivariate analysis, no significant CF were found, and the Harrell's C-index from RF alone was 0.684 with an optimism index of 0.316. The Cox regression models for PFS from the CF + RF of the PreRx/PreBT and Diff are shown in Table 2.

Nomogram

The nomogram from the PFS and DMFS models were developed from the CF + RF model from PreRx and PreBT. For PFS nomogram, variables in the model included FIGO2018 staging (HR 4.197 [95 % CI 1.350, 13.047]), DWIGTVp_PreRx_CentroidZcmValue (HR 0.342 [95 % CI 0.136, 0.865]), DWIGTVp_PreRx_VolumemlValue (HR 2.768 [95 % CI 1.114, 6.877]), and DWIGTVn_PreBT_VolumemlValue (HR 522.512 [95

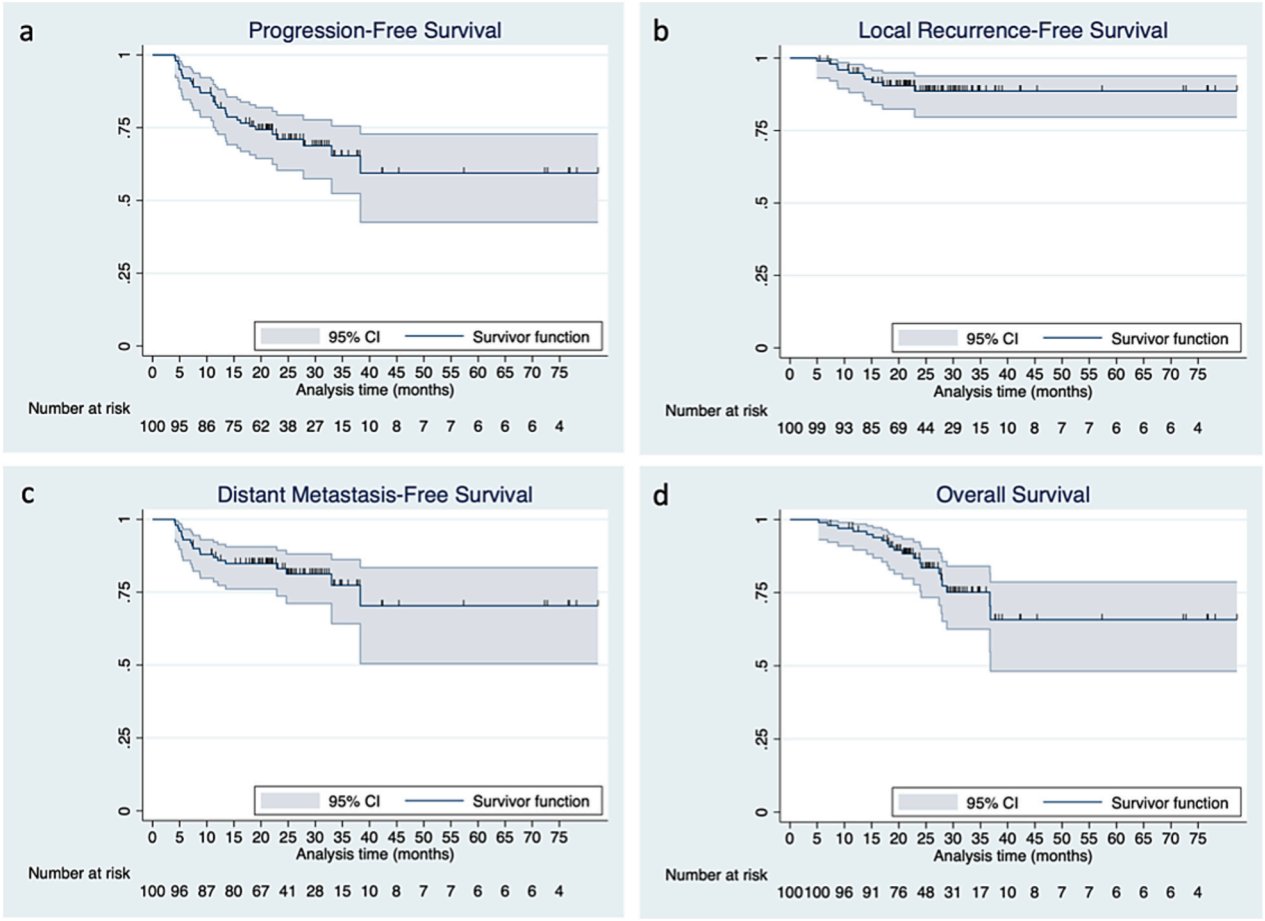

Fig. 2.

% CI 11.971, 22806.708]). For DMFS nomogram, significant predictors were TpreBT (IBS-GEC ESTRO-ABS) (HR 1.311 [95 % CI 1.029, 1.670]), T2GTVp_PreRx_VolumemlValue (HR 0.938 [95 % CI 0.895, 2.448]), T2GTVn_PreBT_VolumemlValue (HR 4.166 [95 % CI 1.627, 5.087]), and DWIGTVn_PreBT_CentroidXcmValue (HR 0.258 [95 % CI 0.100, 1.106]). TpreBT (IBSGEC ESTRO-ABS) or the tumor category during PreBT according to IBS-GEC ESTRO- ABS guidelines[21] had a small effect on the model score. The proposed nomograms predicting PFS and DMFS outcome are shown in Fig. 4a and 4b, respectively.

Discussion

This study aimed to assess the potential of MR radiomics, with or without the combination of clinical factors, in predicting treatment outcomes for patients with LACC. From the multivariate Cox regression analysis, the CF + RF models of the PreRx/PreBT had the highest Harrell's C-index for all outcomes including PFS and OS. The results were similar to those reported by Zhang et al.[21] The results showed that the radiomics score achieved better predictive performance for PFS and OS compared to the FIGO staging system and clinical prediction models. However, in our study, the calibration plots of the models underestimated and overestimated at certain points, suggesting that the model may not be the best fit and that they should be evaluated with a larger sample size for training.

From this study, PreRx and PreBT radiomics appeared to be more predominant to survival outcomes compared to Diff radiomics according to the higher Harrell's C-indices from every model. The possible explanation could be from the large variety of the radiomic values ranging from negative to positive values and from decimals to millions. The Diff from each value might not be a good surrogate. Among the Diff models, RF appeared to have stronger effects compared to CF. Although, there was a study suggesting that RF changed during radiation and that it could be used as a potential predictor to monitor early tumor response [15], the RF changes were not directly compared with the RF at each time point.

Regarding the treatment outcome, in the study cohort, D90 HR-CTV could be achieved with a mean dose of 89.94 Gy ($\alpha/\beta = 10$; Gy10) which is comparable to the 90 Gy reported in the EMBRACE-I trial[2]. This might be due to several methods adopted at the institute to improve the dose coverage of HR-CTV while limiting dose to organs at risk.[4,5,24] However, The patients in this study were 81 % nodal-positive with PAN involvement at 27 %, and 37 % of T2b, and 43 % of T3b which showed less favorable results compared to the patients in the EMBRACE-I trial. Despite harboring a more advanced disease in this study cohort, the survival outcomes were comparable to the previous trial. This study reported 2-years of PFS, LRFS, DMFS, and OS rates of 71, 88.6, 83.1, and 83.5 % respectively.

Our strengths included a homogenous modern radiotherapy treatment scheme from a single institute performing IMRT/VMAT plus 3D-IGABT for the entire cohort. Radiomics from DWI exhibited a more prominent relationship with some clinical outcomes (such as PFS) compared with T2WI. Moreover, RF from GTVp and GTVn were concurrently analyzed, and GTVn emerged as a significant predictor of all outcomes, even LRFS. The addition of PreBT MR images from the PreRx was beneficial in providing more dynamic information during the radiotherapy treatment and made the models more robust. Another strength of this study was the decision to use simple first-order statistics radiomics which could be easily derived from a standard function of MIM® software and allowed more accessibility to radiomics utilizations.

This study also proposed the nomogram for the PFS and DMFS

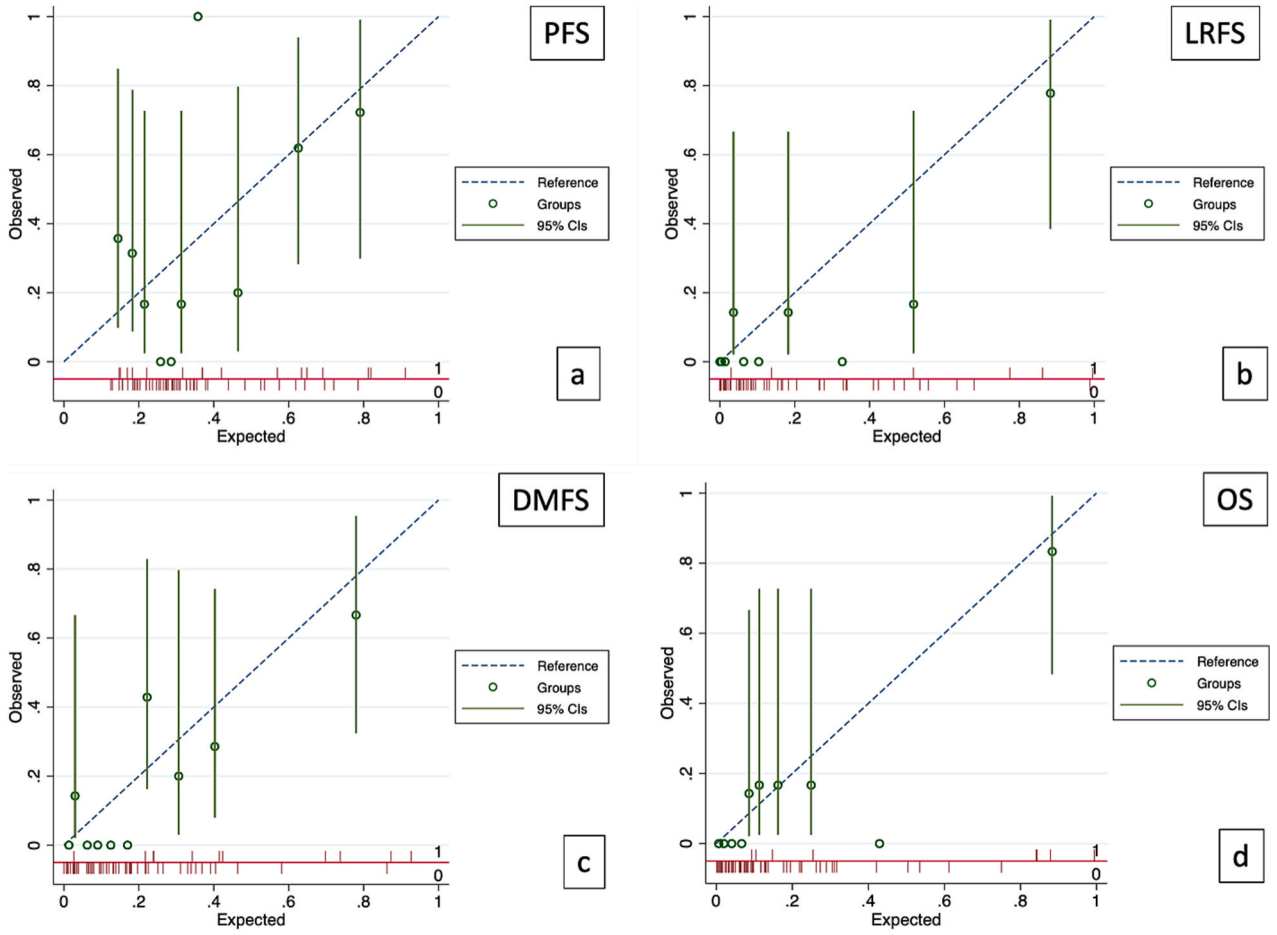

Fig. 3.

derived from the CF + RF of PreRx/PreBT model. Significant CF were FIGO2018 staging and T PreBT was determined according to IBS-GEC ESTRO-ABS recommendations[23], which emphasized the benefit of PreBT MRI to aid in the assessment of the treatment response and benefit radiomics analysis. The proposed nomograms could be a fundamental predictive tool to personalize the treatment for patient with LACC, especially those who would benefit from adjuvant chemotherapy after CCRT. However, further validation of the models and nomograms will be needed before utilization.

However, the retrospective nature of the study could obscure follow-up and events rate.

The small sample size included in the model along with the few events could have affected the model to have over- and underestimation values from calibration plots. A larger sample size in the training cohort could yield more robust models. Another limitation is the limited field length of PreBT which did not cover the whole PAN region. The GTVn which was contoured in this study was limited within only pelvic and groin nodes. Several studies have supported that PAN is a good predictor for distant failure[3,25]. Analyzing PAN radiomics could provide more information to predict DMFS and OS. Moreover, this study only provided internal validation using the Harrell's C- and optimism indices. External validation in future prospective is needed to confirm the accuracy of the models.

Conclusion

RF from the first-order statistics added values to CF to predict the outcomes after CCRT with modern radiotherapy technique in patients with LACC. The highest predictive performance was observed in models combining CF and RF from PreRx and PreBT scans. The proposed nomograms for PFS and DMFS have the potential to guide personalized treatment strategies for patients at high risk of progression and distant relapse post-CCRT. However, further external validation using diverse cohorts is required before these models can be implemented in clinical practice.

This study aimed to investigate the performance of prediction models for clinical factor (CF), radiomic factor (RF), and both factors (CF + RF) combined to measure treatment outcomes in patients with locally advanced cervical cancer (LACC) after concurrent chemoradiation (CCRT) and 3D image-guided adaptive brachytherapy (3D-IGABT).

OS

The median time of death was 24.5 months (IQR 20.1–31.6). Twenty patients died and the rate of OD for 2-years was 83.5 % (95 % CI 73.37–90.02). The Kaplan-Meier curve of OS was shown in Fig. 2d. Univariate Cox regression analysis for PFS is shown in Supplementary Table S5 and S9. The Cox regression CF + RF model from PreRx and PreBT resulted in the highest Harrell's C-index of 0.967 compared to the Harrell's Cindices of the models from RF and CF alone, 0.780 and 0.680, respectively. The optimism index of the CF + RF model was 0.430. The predictive performance from the calibration plot of the CF + RF model from PreRx and PreBT was underestimated when predicting low probabilities and overestimated when predicting high probabilities; however, it was relatively accurate compared to those with other outcomes. The calibration plot is shown in Fig. 3d. For Diff radiomics, Harrell's C-indices from CF + RF was 0.844 with an optimism index of 0.242. The Cox regression models for PFS from CF + RF of PreRx/PreBT and Diff are

Table 2
Cox regression models for PFS [a], LRFS [b], DMFS [c], and OS [d] CF + RF of PreRx/PreBT and Diff.

Cox regression models for PFS from CF + RF of PreRx/PreBT and Diff					
Significant Variables	**HR (95 % CI)**	**P value**	**Significant Variables**	**HR (95 % CI)**	**P value**
Clinical Factors			**Clinical Factors**		
FIGO2018 staging	4.197 (1.350, 13.047)	0.013	None		
Pre-Rx/Pre-BT Radiomic Features			**Difference Radiomic Features**		
DWIGTVp_PreRx_CentroidZcmValue	0.342 (0.136, 0.865)	0.023	DWIGTVn_Diff_CentroidZcmValue	1.112 (1.003, 1.233)	0.044
DWIGTVp_PreRx_VolumemlValue	2.768 (1.114, 6.877)	0.028			
DWIGTVn_PreBT_VolumemlValue	522.512 (11.971, 22806.708)	0.001			
Harrell's C-index	**0.739**		**Harrell's C-index**	**0.588**	
Optimism Index	**0.438**		**Optimism Index**	**0.312**	
Cox regression models for LRFS from CF + RF of PreRx/PreBT and Diff					
Significant Variables	**HR (95 % CI)**	**P value**	**Significant Variables**	**HR (95 % CI)**	**P value**
Clinical Factors			**Clinical Factors**		
Number of Necrotic LN	2.854 (1.539, 5.292)	0.001	None		
Pre-Rx/Pre-BT Radiomic Features			**Difference Radiomic Features**		
T2GTVp_PreBT_VolumemlValue	1.060 (1.027, 1.095)	<0.001	T2GTVp_Diff_MinValue	0.998 (0.996, 1.000)	0.041
T2GTVn_PreBT_CentroidXcmValue	82.926 (6.375, 1078.678)	0.001			
DWIGTVn_PreBT_CentroidXcmValue	0.011 (0.0009, 0.147)	0.001			
Harrell's C-index	**0.873**		**Harrell's C-index**	**0.773**	
Optimism Index	**0.472**		**Optimism Index**	**0.381**	
Cox regression models for DMFS from CF + RF of PreRx/PreBT and Diff					
Significant Variables	**HR (95 % CI)**	**P value**	**Significant Variables**	**HR (95 % CI)**	**P value**
Clinical Factors			**Clinical Factors**		
TpreBT (IBS/GECESTRO)	1.311 (1.029, 1.670)	0.029	None		
Pre-Rx/Pre-BT Radiomic Features			**Difference Radiomic Features**		
T2GTVp_PreRx_VolumemlValue	0.938 (0.895, 2.448)	0.008	T2GTVp_Diff_SphereDiametercmValue	1.062 (1.019, 1.107)	0.004
T2GTVn_PreBT_VolumemlValue	4.166 (1.627, 5.087)	0.003			
DWIGTVn_PreBT_CentroidXcmValue	0.258 (0.100, 1.106)	0.005			
Harrell's C-index	**0.830**		**Harrell's C-index**	**0.684**	
Optimism Index	**0.292**		**Optimism Index**	**0.316**	
Cox regression models for OS from CF + RF of PreRx/PreBT and Diff					
Significant Variables	**HR (95 % CI)**	**P value**	**Significant Variables**	**HR (95 % CI)**	**P value**
Clinical Factors			**Clinical Factors**		
HR-CTV volume at 1st brachytherapy	1.019 (1.005, 1.033)	0.007	T staging	210.623 (3.131, 14168.040)	0.013
Maximum short axis LN (cm)	8.287 (2.295, 29.917)	0.001	Maximum short axis LN (cm)	128.852 (1.583, 10486.88)	0.030
Number of Necrotic LN	3.608 (1.214, 10.723)	0.021			
Pre-Rx/Pre-BT Radiomic Features			**Difference Radiomic Features**		
T2GTVp_PreRx_VolumemlValue	14.598 (4.052, 52.589)	<0.001	T2GTVn_Diff_KurtosisValue	0.115 (0.002, 0.750)	0.024
DWIGTVp_PreBT_MinValue	0.995 (0.992, 0.997)	<0.001	T2GTVn_Diff_SkewnessValue	0.025 (0.001, 0.651)	0.027
DWIGTVp_PreBT_VolumemlValue	3.360 (1.235, 9.138)	0.018			
T2GTVn_PreBT_MaxValue	1.545 (1.245, 1.918)	<0.001			
Harrell's C-index	**0.967**		**Harrell's C-index**	**0.844**	
Optimism Index	**0.430**		**Optimism Index**	**0.242**	

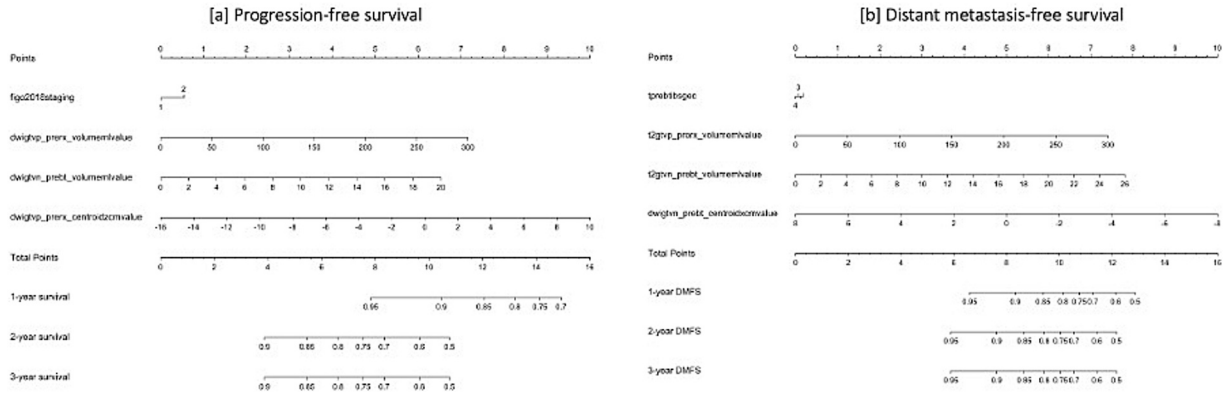

Fig. 4.

shown in Table 2.

CRediT authorship contribution statement

Wiwatchai Sittiwong: Conceptualization, Data curation, Investigation, Methodology, Formal analysis, Project administration, Writing – original draft. **Pittaya Dankulchai:** Conceptualization, Methodology, Project administration, Writing – review & editing. **Pitchayut Wongsuwan:** Conceptualization, Data curation, Investigation, Formal analysis, Methodology, Resources, Writing – original draft. **Tissana Prasartseree:** Conceptualization, Methodology, Investigation, Writing – review & editing. **Wajana Thaweerat:** Conceptualization, Methodology, Investigation, Writing – review & editing. **Nerisa Thornsri:** Conceptualization, Methodology, Formal analysis. **Pongpop**

Tuntapakul: Conceptualization, Methodology, Investigation, Writing – review & editing.

Declaration of Competing Interest

The authors declare that they have no known competing financial interests or personal relationships that could have appeared to influence the work reported in this paper.

Appendix A. Supplementary data

Supplementary data to this article can be found online at https://doi.org/10.1016/j.ctro.2025.100965.

References

[1] Sturdza A, Potter R, Fokdal LU, Haie-Meder C, Tan LT, Mazeron R, et al. Image guided brachytherapy in locally advanced cervical cancer: Improved pelvic control and survival in RetroEMBRACE, a multicenter cohort study. Radiother Oncol 2016; 120(3):428–33.

[2] Potter R, Tanderup K, Schmid MP, Jurgenliemk-Schulz I, Haie-Meder C, Fokdal LU, et al. MRI-guided adaptive brachytherapy in locally advanced cervical cancer (EMBRACE-I): a multicentre prospective cohort study. Lancet Oncol 2021;22(4): 538–47.

[3] Tan LT, Potter R, Sturdza A, Fokdal L, Haie-Meder C, Schmid M, et al. Change in Patterns of Failure After Image-Guided Brachytherapy for Cervical Cancer: Analysis From the RetroEMBRACE Study. Int J Radiat Oncol Biol Phys 2019;104(4): 895–902.

[4] Dankulchai P, Harn-Utairasmee P, Prasartseree T, Nakkasae P, Trikhirhisthit K, Sittiwong W, et al. Vaginal 11-point and volumetric dose related to late vaginal complications in patients with cervical cancer treated with external beam radiotherapy and image-guided adaptive brachytherapy. Radiother Oncol 2022; 174:77–86.

[5] Prasartseree T, Dankulchai P, Hoskin PJ. Excess dose-related parameters (Vex, Rex, and iRex): novel predictors and late toxicity correlations in cervical cancer imageguided adaptive brachytherapy. J Contemp Brachytherapy 2020;12(5): 441–53.

[6] Mileshkin LR, Moore KN, Barnes EH, Gebski V, Narayan K, King MT, et al. Adjuvant chemotherapy following chemoradiotherapy as primary treatment for locally advanced cervical cancer versus chemoradiotherapy alone (OUTBACK): an international, open-label, randomised, phase 3 trial. Lancet Oncol 2023;24(5): 468–82.

[7] Duenas-Gonzalez A, Zarba JJ, Patel F, Alcedo JC, Beslija S, Casanova L, et al. Phase III, open-label, randomized study comparing concurrent gemcitabine plus cisplatin and radiation followed by adjuvant gemcitabine and cisplatin versus concurrent cisplatin and radiation in patients with stage IIB to IVA carcinoma of the cervix. J Clin Oncol 2011;29(13):1678–85.

[8] Lorusso D, Xiang Y, Hasegawa K, Scambia G, Leiva M, Ramos-Elias P, et al. Pembrolizumab or placebo with chemoradiotherapy followed by pembrolizumab or placebo for newly diagnosed, high-risk, locally advanced cervical cancer (ENGOT-CX11/gog-3047/keynote-A18): A randomized, double-blind, phase 3 clinical trial. Obstet Gynecol Surv 2024 Sept;;79(9):523–4.

[9] 10. McCormack M, Eminowicz G, Gallardo D, Diez P, Farrelly L, Kent C, et al. Induction chemotherapy followed by standard chemoradiotherapy versus standard chemoradiotherapy alone in patients with locally advanced cervical cancer (GCIG interlace): An international, Multicentre, randomised phase 3 trial. Lancet 2024 Oct;404(10462):1525–35.

[11] Chen HH, Meng WY, Li RZ, Wang QY, Wang YW, Pan HD, et al. Potential prognostic factors in progression-free survival for patients with cervical cancer. BMC Cancer 2021;21(1):531.

[12] Thephamongkhol K, Korpraphong P, Muangsomboon K, Sitathanee C, Lertkhachonsuk AA, Phongkitkarun S, et al. Development and validation of a prognostic prediction model including the minor lymphatic pathway for distant metastases in cervical cancer patients. Sci Rep 2022;12(1):9873.

[13] Jiang K, Ai Y, Li Y, Jia L. Nomogram models for the prognosis of cervical cancer: A SEER-based study. Front Oncol 2022;12:961678.

[14] Gui B, Autorino R, Micco M, Nardangeli A, Pesce A, Lenkowicz J, et al. Pretreatment MRI Radiomics Based Response Prediction Model in Locally Advanced Cervical Cancer. Diagnostics (basel) 2021;11(4).

[15] Meng J, Zhu L, Zhu L, Wang H, Liu S, Yan J, et al. Apparent diffusion coefficient histogram shape analysis for monitoring early response in patients with advanced cervical cancers undergoing concurrent chemo-radiotherapy. Radiat Oncol 2016; 11(1):141.

[16] Shur JD, Doran SJ, Kumar S, Ap Dafydd D, Downey K, O'Connor JPB, et al. Radiomics in Oncology: A Practical Guide. Radiographics 2021;41(6):1717–32.

[17] Kang CY, Duarte SE, Kim HS, Kim E, Park J, Lee AD, et al. Artificial Intelligencebased Radiomics in the Era of Immuno-oncology. Oncologist 2022;27 (6):e471–83.

[18] Limkin EJ, Sun R, Dercle L, Zacharaki EI, Robert C, Reuze S, et al. Promises and challenges for the implementation of computational medical imaging (radiomics) in oncology. Ann Oncol 2017;28(6):1191–206.

[19] Small C, Prior P, Nasief H, Zeitlin R, Saeed H, Paulson E, et al. A general framework to develop a radiomic fingerprint for progression-free survival in cervical cancer. Brachytherapy 2023;22(6):728–35.

[20] Schmid MP, Lindegaard JC, Mahantshetty U, Tanderup K, Jurgenliemk-Schulz I, Haie-Meder C, et al. Risk Factors for Local Failure Following Chemoradiation and Magnetic Resonance Image-Guided Brachytherapy in Locally Advanced Cervical Cancer: Results From the EMBRACE-I Study. J Clin Oncol 2023;41(10):1933–42.

[21] Zhang X, Zhao J, Zhang Q, Wang S, Zhang J, An J, et al. MRI-based radiomics value for predicting the survival of patients with locally advanced cervical squamous cell cancer treated with concurrent chemoradiotherapy. Cancer Imaging 2022;22(1): 35.

[22] Ikushima H, Haga A, Ando K, Kato S, Kaneyasu Y, Uno T, et al. Prediction of out-of-field recurrence after chemoradiotherapy for cervical cancer using a combination model of clinical parameters and magnetic resonance imaging radiomics: a multiinstitutional study of the Japanese Radiation Oncology Study Group. J Radiat Res 2022;63(1):98–106.

[23] Mahantshetty U, Poetter R, Beriwal S, Grover S, Lavanya G, Rai B, et al. IBSGEC ESTRO-ABS recommendations for CT based contouring in image guided adaptive brachytherapy for cervical cancer. Radiother Oncol 2021;160:273–84.

[24] Dankulchai P, Lohasammakul S, Petsuksiri J, Nakkrasae P, Tuntipumiamorn L, Kakanaporn C, et al. Dosimetric analysis and preliminary clinical result of image-guided brachytherapy with or without hybrid technique for cervical cancer using VariSource titanium ring applicator with "Siriraj Ring Cap". Brachytherapy 2017; 16(6):1199–204.

[25] Shylasree TS, Gurram L, Das U. Para-aortic lymph node involvement in cervical cancer: Implications for staging, outcome and treatment. Indian J Med Res 2021; 154(2):267–72.

[26] Dankulchai P, Thanamitsomboon N, Sittiwong W, et al. Pre-treatment T2-weighted magnetic resonance radiomics for prediction of loco-regional recurrence after image-guided adaptive brachytherapy for locally advanced cervical cancer. J Contemp Brachytherapy 2024;16(3):193–201. https://doi.org/10.5114/jcb.2024.141458.